INŻYNIERIA MINERALNA

2(52) 2023

CZASOPISMO POLSKIEGO TOWARZYSTWA PRZERÓBKI KOPALIN

NR 2(52) 2023, LIPIEC – GRUDZIEŃ

PL ISSN 1640 - 4920

JOURNAL OF THE POLISH MINERAL ENGINEERING SOCIETY

NO. 2(52) 2023, JULY – DECEMBER

Numerical Study on Effects of Airflow Parameters on the Air Temperature the at Mechanized Longwall of Mongduong Coal Mine

Hong NGUYEN THI[1], Quang NGUYEN VAN[2]

[1] Faculty of Environment, Hanoi University of Mining and Geology, 18 Vien street, Hanoi, Vietnam; email: nguyenthihong@humg.edu.vn
[2] Faculty of Mining, Hanoi University of Mining and Geology, 18 Vien street, Hanoi, Vietnam; email: quangnv@humg.edu.vn

http://dot.org/10.29227/IM-2023-02-16

Submission date: 26-08-2023 | Review date: 21-09-2023

Abstract

The increasing depth of extraction and the degree of mechanization leading to the risk of workers working in poor microclimate conditions has become one of the major safety issues in coal mines. During the survey of the current microclimate in Mongduong coal mine, it showed that the temperature of the mechanized longwall exceeded the permissible regulations (t°< 30°C), the air humidity is about 95–100%. The reason for the increase of air temperature in longwall is due to geothermal, heat radiated from the longwall equipment and the inlet wind high temperature. To improve the thermal environment in the mechanized longwall area, Vietnam's coal mines open use ventilation, but the efficiency is not high. Therefore, the paper evaluated the influence of airflow on the temperature of the longwall, 7 models with different air flow velocities and 3 models with inlet air temperature have been created in ICM-CFD and simulated by Ansys CFX software. The environment temperature of each model was evaluated by analyzing the average temperature of the roadway section, the cross-section distribution of the roadway temperature and the velocity streamline of the whole roadway. As a result, the air flow rate increases leading to the air temperature in the longwall decreases, however the wind speed is limited. The inlet temperature of the gas stream is an important factor that affects the thermal environment in the longwall. The results of the article are the basis for making solutions to improve the thermal environment suitable for high-temperature longwall.

Keywords: *numerical modelling, Ansys CFX, mechanized longwall, temperature of air mine, velocity of air mine, Mongduong coal mine*

1. Introduction

Coal serves as an indispensable energy source for the development of domestic economies, providing fuel for power plants and various industries. However, this vital resource is being rapidly depleted at shallow levels, pushing mining operations to exploit deeper reserves. Such deep-level mining poses potential risks to labor safety and can significantly impact the microclimate in underground coal mines. In recent years, several coal mines in Quang Ninh, Vietnam, particularly the Mong Duong Coal Mine's L7 longwall, have undergone deep mining operations and adopted mechanized techniques, resulting in elevated air temperatures within the mining areas. The soaring air temperatures in the L7 longwall region, for instance, have been observed to exceed the standard QCVN 01/2011/BCT [Ministry of Industry and Trade, 2011], surpassing 30°C. Prolonged exposure of workers to such high-temperature environments poses potential health risks to miners, compromising mining efficiency (He and Guo 2013; Yang et al. 2011), and increasing the frequency of accidents while decreasing labor productivity. Among the primary causes of rising mine air temperatures are the heat emitted from surrounding rocks and electrical equipment, along with the oxidation of coal (He et al. 2010; Su et al. 2009). Previous studies, such as those conducted by [Dao Van Chi et al., 2019] and [Quan Truong Tien et al., 2019], have explored the factors influencing temperature increase, including soil, rock, and coal temperatures. Additionally, the study of mine airflow indicates that the primary source of heat is the surrounding rock, particularly the rock surfaces near the work face (Zhang et al. 2017; Maurya et al. 2015), and the temperature of the air flow is closely linked to the airflow path, which is influenced by the ventilation system (Su et al. 2017; Hua et al. 2018). In this study, we aim to analyze the main heat sources in the L7 longwall mining area of Mong Duong coal mine and establish a numerical model to explore the relationship between various parameters and the temperature distribution in the longwall area. Specifically, we consider wind velocity parameters (V = 0.5 m/s, 1 m/s, 1.5 m/s, 2 m/s, 2.5 m/s, 3 m/s, 3.5 m/s, 4 m/s) and variations in inlet wind temperature (T = 29°C, 26°C, 24°C). By investigating these factors, our research endeavors to provide valuable insights into the heat dynamics of deep-level coal mining areas, offering a foundation for effective strategies in managing and mitigating excessive air temperatures, thereby enhancing worker safety and overall mining productivity.

2.Heat sources affecting mine air temperature

2.1 Radiative heat from surrounding rock

The difference between the initial temperature of the surrounding rock and the airflow in the shaft determines the heat exchange driving force. A positive or negative temperature difference governs the direction of heat transfer between the surrounding rock and the air. Due to the significant temperature gradient in the ground, the initial rock temperature is typically higher than the temperature of the airflow in the tunnel, making the surrounding rock a crucial heat source for the tunnel walls. In deep mines, the heat flux value can be considerable, often surpassing the total heat flux from other sources, due to the influence of the initial rock temperature. The convective heat transfer between the surrounding rock and the airflow is an unstable heat transfer process. The temperature of the surrounding rock in the well is higher due to the impact of ground heat flow, leading to an unstable transmission of heat flux. Over time, the radius of the surrounding

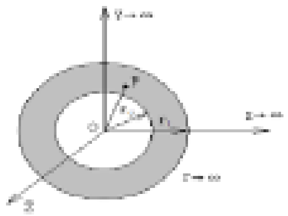

Fig. 1. Diagram of the cylindrical surface of an infinitesimal object

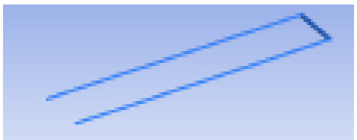

Fig. 2. Model of the longwall area using ICEM – CFD

rock's thermal adjustment zone increases, and the heat flow source expands into the deeper rock layers. Through observation and theoretical analysis, it becomes evident that once the tunnel ventilation reaches a certain duration, the convective heat transfer between the surrounding rock and the axial airflow stabilizes, allowing the heat exchange between them to be considered as stable [Вороnаев.А.ф, 1961].

$$Q_r = K_t U.L(t_x - t),\ kW \qquad (1)$$

Q_r – Radiator from surrounding rock, kW
K_t – Unstable heat transfer coefficient from surrounding rock
U – Road circumference, m
L – Road length
t_x – Initial temperature at depth x, °C
t – The average temperature of the airflow, °C

In order to calculate the heat transfer between the surrounding rock and the airflow, the following assumptions are commonly employed:

The rock temperature is uniform and equal to the initial rock temperature along the entire roadway circumference. The heat transfer conditions remain consistent, and the air inside the roadway maintains a constant temperature. All heat from the surrounding rock is transferred to the airflow..

Following ventilation of the roadway, a heat exchange process ensues between the surrounding rock and the airflow. The heat from the surrounding rock is transferred to the airflow, leading to cooling of the surrounding rock and subsequent changes in its temperature field over time. Consequently, the thermal conduction of the surrounding rock becomes an unstable heat conduction process in the Cartesian coordinate system., that is:

$$T = T(x,y,z,t) \qquad (2)$$

According to the two basic laws of heat transfer, namely the law of conservation of heat and Fourier's law of thermal conduction, the basic equation of three-dimensional heat conduction can be established. This equation, serves as a fundamental framework for analyzing heat flow and temperature distribution in three-dimensional systems: [Liu Shishi, et al 1994]

$$\frac{\partial T}{\partial t} = \alpha\left(\frac{\partial^2 T}{\partial x^2} + \frac{\partial^2 T}{\partial y^2} + \frac{\partial^2 T}{\partial z^2}\right) \qquad (3)$$

where a is the temperature coefficient of the surrounding rock, m^2/s.

$$\alpha = \frac{\lambda}{c\rho} \qquad (4)$$

Where:
c – is the specific heat capacity of the rock, J/(kg · °C);
ρ – is the density of rock, kg /m³;
λ – is the thermal conductivity of the rock, kW/m °C.

In the Cartesian coordinate system, the heat transfer in the surrounding rock can be conceptualized as a two-dimensional unstable heat conduction process. To simplify the analysis, we convert the Cartesian coordinate system into a cylindrical coordinate system and thereby transform the two-dimensional heat conduction equation for the surrounding rock into a more manageable one-dimensional heat conduction equation

$$\frac{\partial T}{\partial t} = \alpha\left(\frac{\partial^2 T}{\partial x^2} + \frac{\partial^2 T}{\partial y^2}\right) \qquad (5)$$

Set up temperature to T (r, τ), $r = (x^2 + y^2)^{1/2}$:

$$\frac{\partial T}{\partial t} = \alpha\left(\frac{\partial^2 T}{\partial r^2} + \frac{1}{r}\frac{\partial T}{\partial r^2} + \frac{1}{r^2}\frac{\partial^2 T}{\partial \theta^2}\right) \qquad (6)$$

Since T is independent of θ, temperature distribution T (r, τ) satisfy the equation

$$\frac{\partial T}{\partial t} = \alpha\left(\frac{\partial^2 T}{\partial r^2} + \frac{1}{r}\frac{\partial T}{\partial r}\right) \qquad (7)$$

Its mean:

$$\frac{\partial^2 T}{\partial r^2} + \frac{1}{r}\frac{\partial T}{\partial r^2} + \frac{1}{a}\frac{\partial T}{\partial t} = 0\ (6)\ r_0 < r < \infty,\ t > 0 \qquad (8)$$

The initial conditions:

$$r_0 \le r < +\infty,\ t = 0,\ T(r,0) = t_0 = t_y = const \qquad (9)$$

The boundary condition is: when khi τ > 0, r = r_o. When the surrounding rock and convection heat dissipation path h is the

Tab. 1. Parameters in the model

Parameters of the longwall	Model parameters	Parameters of the longwall	Model parameters
velocity	1 m/s; 1,5 m/s; 2m/s; 2,5m/s; 3m/s; 3,5 m/s; 4m/s	Temperature of equipment	308,15K ~ 311,15K
outlet	outlet	roughness	2 cm
Temperature air of inlet	297,15K; 299,15K; 302,15K;	Thermal conductivity of rock	1,9 W/mk
Initial air of temperature	302,15K	Thermal conductivity of coal	0,35W/k
Temperature of rock	304,15K ~ 305,15K		

surrounding rock and the convective heat transfer coefficient of the wind flow. tf is the dry bulb temperature of the wind.

$$\lambda.\frac{\partial T}{\partial r} = h\left(T - t_f\right) \tag{10}$$

When $\tau > 0, r \to \infty$, The surrounding rock temperature is equal to the original rock temperature, mean: $T(\infty, t) = t_y = const$.

2.2. Heat dissipation of electromechanical equipment

As the mechanization level improves and mining capacity increases in underground coal mines, the microclimate conditions of the mine are also affected. Generally, the electrical energy supplied to electromechanical devices on the charging line can be divided into two parts: useful work and thermal energy. During the operation of electromechanical equipment, kinetic energy is relatively small, and the primary useful work involves lifting materials to the surface, increasing the potential energy of the material or liquid. However, any excess electrical energy not utilized for useful work is converted into thermal energy, nearly all of which is dissipated into the tunnel airflow. Investigating the thermal release of electromechanical equipment mainly involves examining its rated power and mechanical efficiency (1). By utilizing the appropriate calculation coefficients, the heat dissipation provided by the engine to the airflow can be calculated as shown in [Wu Zhongli, 1989].

$$Q_n = 3600.\eta_n.N\ ,\ KJ/h \tag{11}$$

In here:
3600 is the power of 1k W which is equivalent to the heat of 3600k J/h;
N is the power of the motor, k W;

2.3 Heat dissipation during coal transportation

The heat dissipation of coal during transport is, in fact, another manifestation of the heat dissipation from the surrounding rock. This aspect holds significant importance in understanding the transfer of heat and moisture in modern mines. As a result, the temperature of the surrounding airflow increases, [Yan Ronglin et al,2004]

$$Q_k = m_k.k.C_k.\Delta t_k.kw \tag{12}$$

Where: Q_k – is the heat dissipation of coal transportation, Kw
m_k – is the amount of coal transportation, kg/s;
C_k – is the average specific heat of coal transportation., kJ/kg.^{0}c
Δt_k – is the temperature at which coal is cooled in the road section under consideration during transportation, ^{0}C.

Similar to soil, the temperature of coal also increases with the depth of exploitation and exceeds the temperature of the underground air during the initial period. Consequently, the heat transfer process between coal and air during transportation becomes a critical factor to consider.

3. Model

3.1. Model Construction

The model is based on the characteristics of the L7 mechanized longwall at the Mong Duong coal mine, which is exploited at a depth of -250/-160 meters and has a yearly capacity of 300 thousand tons. The mining process involves the MG160/380 machine code in combination with support from the ZF3000/15/24 code. The transportation is facilitated by the SZZ-110KW Conveyor and the SGZ-220KW Tractor, while the coal is crushed using the PLM500 90KW Crusher. The mining operation operates in two shifts, with an additional preparation shift. The dimensions of the longwall are as follows: a length of 120 meters, a width of 6 meters, and a height of 2.2 meters. The thickness of the coal seam is 5.5 meters, and the cross-sectional area of the roadway is 13m^2, extending over a length of 350 meters. Temperature survey results indicate that the average temperature along the transport seam of the roadway ranges from 302.5K to 304.65K, while the average temperature of the longwall ranges from 304.15K to 305.15K. In this study, a model is developed to analyze the influence of wind velocity parameters and changes in inlet wind temperature on the temperature distribution. The wind velocity parameters considered in the model are: v = 0.5 m/s, 1 m/s, 1.5 m/s, 2 m/s, 2.5 m/s, 3 m/s, 3.5 m/s, and 4 m/s. Additionally, variations in the inlet wind temperature are examined, specifically at Tn = 29°C, 26°C, and 24°C. By utilizing this model, we aim to gain valuable insights into the heat distribution within the longwall mining area, and understand how changes in wind velocity and inlet wind temperature can impact the overall temperature conditions during the mining process.

3.2. Numerical Model

For the numerical analysis, the article employs Computational Fluid Dynamics (CFD) through numerical simulation. The geometric modeling and meshing of the model are conducted using ICEM-CFD software, maintaining the same geometric dimensions as mentioned earlier. The mesh consists of approximately 3x106 to 3.6x106 elements. The boundary conditions are categorized into two classes. The numerical simulation is performed in CFX, utilizing the K-ε turbulence model. This model is chosen for its ability to provide accurate predictions of turbulence, making it suitable for analyzing the airflow patterns and heat transfer within the longwall mining area.

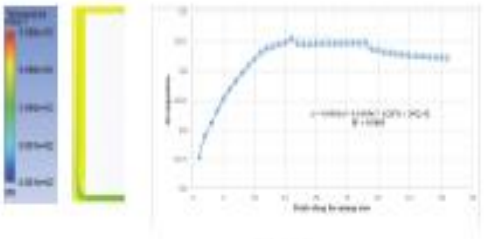

V = 1 m/s

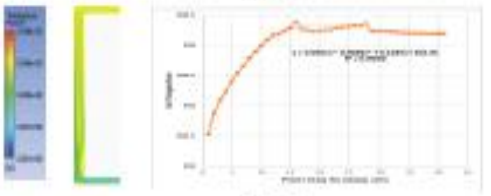

V = 1.5 m/s

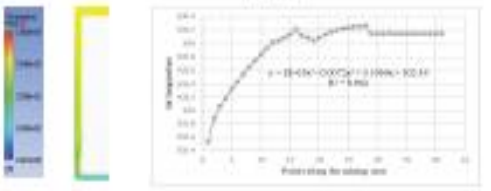

V = 2 m/s

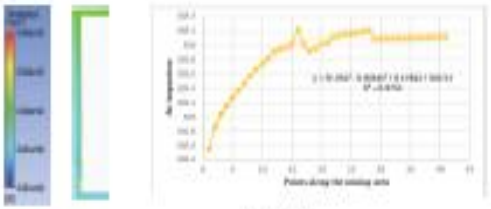

V = 2.5 m/s

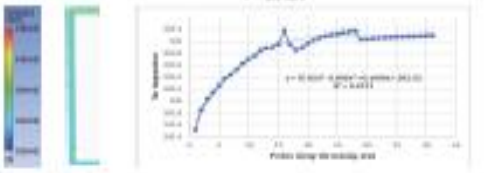

V = 3 m/s

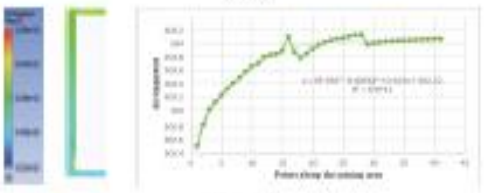

V = 3.5 m/s

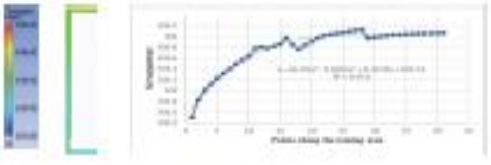

V = 4m/s

Fig. 2. Temperature field and trend of temperature change along the mining area

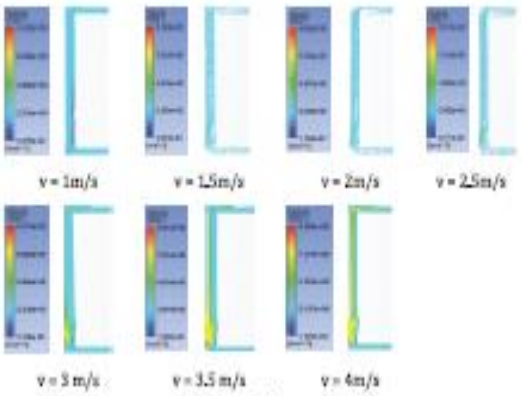

Fig. 3. Velocity field at mining area

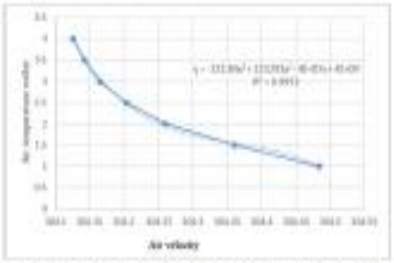

Fig. 4. Relationship between wind speed and air temperature of longwall

3.3. Mathetical model

The heat exchange between the rock and air is calculated using the conservation equations for mass, momentum, and energy. To simulate these phenomena related to the flow of liquid and gas, heat transfer, and mass, Computational Fluid Dynamics (CFD) is employed in this study. CFD is a powerful numerical method used to analyze and predict various fluid-related processes. In this paper, CFD is utilized to investigate the impact of parameters such as duct position and inlet temperature on the temperature distribution in the work area. The model considers a turbulent flow of viscous incompressible gas, and the mathematical equations from fluid mechanics form the foundation for solving problems associated with gas transport.

1. The continuity equation

$$\frac{\partial \rho}{\partial t} + \frac{\partial(\rho u)}{\partial x} + \frac{\partial(\rho v)}{\partial y} + \frac{\partial(\rho w)}{\partial z} = 0$$

Where: u,v,w direction velocity (m/s); ρ density (kg/m^3); t: time (s)

2. The momentum equation

$$\frac{\partial}{\partial t}(\rho v) + \nabla.(\rho v) = -\nabla p + \nabla T + \rho g + F$$

Where: p is static pressure (pa) T - stress tensor (pa), gravitationnal body force (m/s^2); F external body force (N);

3. The energy equation

$$\frac{\partial}{\partial t}(\rho E) + \nabla.[v(\rho E + p)] = \nabla(k_{eff}\nabla T) + S_h$$

Where: E: energy (J), T temperature (K); k_{eff} effective thermal conductivity; S_h source term.

3.4. Boundary conditions

The boundary conditions and computational model settings for this study are presented in table 1.

4. Results and discussion

4.1. Effect of airflow rate

The simulation results are shown in Figure 3-6. Fig. 2 displays the airflow temperature field in the working area under different ventilation rates. The temperature distribution along the horizontal section of the roadway appears to be uniform. However, in the longwall, the temperature distribution exhibits significant variation. Notably, a high-temperature region emerges near the corner at the bottom of the longwall, and as the inlet wind speed increases, this high-temperature area gradually expands. The influence of eddy currents plays a role in increasing the heat exchange time and heat dissipation of the cutter when it operates at the bottom of the longwall, resulting in a more uniform temperature distribution in that region. Conversely, for wind speeds exceeding v > 2 m/s, more eddy currents are generated at the top and bottom of the longwall, leading to a more fluctuating temperature distribution at the top and creating a high-temperature region. The simulation results enable the establishment of a relationship between the mine air temperature along the mining area, depicted through a nonlinear regression function of order 3. This relationship provides a basis for forecasting the temperature of the mining area as the wind speed varies. These findings are crucial for understanding the heat distribution and airflow dynamics within the longwall mining area. Moreover, they facilitate accurate predictions of temperature changes with varying wind speeds, enhancing safety and efficiency in mining operations.

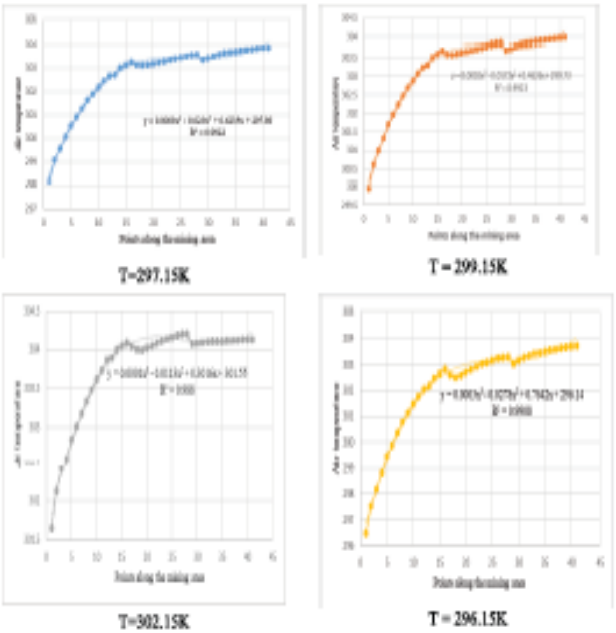

Fig. 5. Trends in air temperature variations along the mining area with different input temperatures

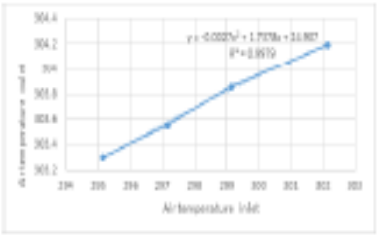

Fig. 6. The relationship between input and output temperature in the longwall

Fig. 3 illustrates the velocity field at the mining area. The figure reveals that the wind velocity field on the horizontal section along the roadway remains relatively stable. However, significant fluctuations in velocity are observed at the bottom and top of the longwall, creating distinct vortex patterns when the wind speed increases.

As the inlet wind speed increases, the area of the vortex expands gradually, promoting convective heat transfer between the wind flow and the high-temperature regions. Notably, at the bottom and top of the longwall, the wind speed towards the wall is higher, resulting in a wider area of influence. Conversely, on the lower side, the wind speed is lower, leading to localized temperature increases. These observations provide valuable insights into the airflow dynamics within the longwall mining area. The presence of vortices and their behavior with varying wind speeds play a significant role in the convective heat transfer process. Understanding these phenomena is crucial for optimizing ventilation strategies and enhancing the overall heat dissipation efficiency within the mining area. By accurately assessing the velocity field, miners can mitigate potential risks associated with localized temperature variations, ensuring safer and more productive mining operations.

Fig. 4 presents the relationship between wind speed and air temperature of the longwall. The airflow rate plays a crucial role in influencing the microclimate conditions within the mining area. Variations in airflow rate can significantly impact the heat distribution and temperature levels in the working environment. Through numerical simulations and field measurements, the study investigates the effect of different airflow rates on the temperature distribution along the longwall. The results reveal that as the airflow rate increases, there is a corresponding decrease in the air temperature within the longwall area. The relationship between airflow rate and longwall temperature is found to be nonlinear, and it is effectively represented by a third-order nonlinear regression function. The findings highlight the importance of carefully controlling the airflow rate to maintain an optimal working environment. By understanding the impact of airflow rate on the microclimate conditions, mining operations can implement effective ventilation strategies to ensure the safety, comfort, and productivity of workers in the mining area. Moreover, the results provide valuable data for forecasting temperature changes and optimizing ventilation systems in modern mines.

4.3. Effects of inlet air temperature

Tab. 2. Temperature measurement and simulation results

Distance to face (m)	Measurement data (°C)	Simulation data (°C)	errors (°K)	Distance to face (m)	Measurement data (°C)	Simulation data (°C)	errors (°K)
Roadway transport				Longwall			
5	30,5	30,378	-0,12	5	31,1	31,099	0
60	29,7	29,868	0,17	10	31,8	31,729	-0,07
120	30,3	30,305	0,01	20	31	31,031	0,03
180	30,1	30,014	-0,09	40	31,4	31,388	-0,01
240	30,6	30,748	0,15	60	31,8	31,697	-0,10
300	30,7	30,947	0,25	90	31,5	31,466	-0,03
340	30,8	31,041	0,24	115	31,4	31,211	-0,19
Ventilation roadway							
5	31,4	31,09	-0,31	340	31,8	31,831	0,03
60	31,5	31,082	-0,42	300	31,7	31,845	0,15
120	31,2	31,009	-0,19	240	31,6	31,839	0,24
180	31	31,06	0,06				

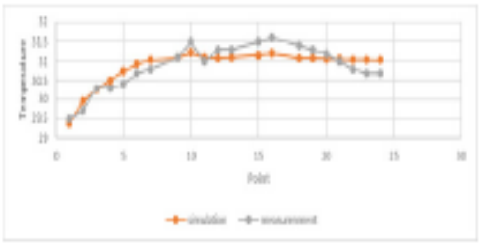

Fig. 7. Measurement and simulation results

From the model above, change the input temperature parameter T= 297.15 K ; 299.15K ; 302.15K, with v =1.5 m/s according to mine parameters. The results are presented in Fig. 5.

From the results in Figure 5, it can be observed that changes in the input temperature significantly affect the temperature along the mining area. The temperature gradually increases along the roadway and the longwall. The temperature variations along the longwall exhibit a cubic nonlinear trend. For the model with T=297.15K, the air temperature within the mine remains below 303.5K. However, for the models with T=299.15K and T=302.15K, the air temperature within the mining area exceeds the standard specified in QCVN 01/2011/BCT, which can impact labor productivity and the health of the workers. Additionally, Figure 6 illustrates the relationship between the input air temperature from the starting point of the transportation roadway and the output temperature of the longwall at the starting point of the longwall. This relationship is represented by a nonlinear regression function. The input temperature has a substantial impact on the temperature in the longwall area. It is crucial to implement solutions to reduce the temperature in the longwall area, ensuring the safety and well-being of the workers. Overall, these findings emphasize the importance of controlling and optimizing the microclimate conditions within the longwall mining area to ensure a safe and healthy working environment for the workers.

4.4. Check the fit of the model

The measured objects are the air parameters in the area of the L7 mechanized longwall, Mongdaong coal mine.measurements of air velocity and roadway cross-sectional area, air temperature. Measuring instruments : Anemometer PMA-2008; Psychrometer Assmann. Measurements are taken at measuring points along the along roadway the transport with a distance from the inlet point general response l =5m, 60m, 120m, 180m, 240m, 300m, 340m. along longwall with a distance from the inlet point are l= 5m, 10m, 20m, 40m, 60m, 90m, 115m.The measuring points along ventilation roadway are l =5m, 60m, 120m, 180m, 240m, 300m, 340m.

Figure 7 presents the numerical simulation results of the model with a wind velocity of v = 2 m/s. A comparison with the field measurements indicates slight deviations between the two sets of data, but these differences do not significantly impact the accuracy of the numerical simulations. Hence, the results obtained from the numerical simulations remain reliable and hold substantial reference value.

5. Conclusion

In conclusion, the survey results and model building based on the actual parameters of the L7 mechanized longwall in Mong Duong coal mine have highlighted the significant influence of geothermal heat and heat generated from mining equipment, as well as the inlet air temperature of the coal mine. Under the same mining conditions, the input temperature and inlet wind speed have a nonlinear relationship with the temperature in the longwall. The simulation results demonstrate that changes in wind speed follow an increasing trend, leading to a reduction in the air temperature in the mining area. However, it is observed that this temperature difference tends to decrease to a certain value as the wind speed increases further. At that point, the wind will no longer be effective in reducing the temperature of the longwall. Therefore, for high-temperature mine areas, it is advisable to implement strategies such as increasing the wind speed and reducing the inlet air temperature to ensure more favorable working conditions for the workers. Measures should be taken to regulate the temperature of the inlet wind during deep mining operations, and the use of air conditioners in the mines is recommended to maintain microclimate conditions in accordance with regulations and create a comfortable environment for the workers. By implementing these measures, mining operations can ensure the safety, health, and well-being of the workers and promote more efficient and productive mining activities. The optimization of ventilation and temperature control strategies is crucial for the successful and sustainable operation of the mine.

Literatura – References

1. ВоронаеnА.ф. управлениИе тоодонаМ Ромнтот ЯгаУгоожжигаз.М. ГомоРтозиздат. 1961.
2. Dao Van Chi , Le Van Thao, 2019. Research on solutions to prevent coal seam temperature rise in mechanized transport kilns area 7.3.1 zone I seam 7 Ha Lam coal mine. Mining Industry Journal. Number 4, page 66-:68 and page 99.
3. He M, Cao X, Xie Q, Yang J, Qi P, Yang Q, Chen X (2010) Principles and technology for stepwise utilization of resources for mitigating deep mine heat hazards. Int J Min Sci Technol 20:20–27
4. He M, Guo P (2013) Deep rock mass thermodynamic effect and temperature control measures. Chin J Rock Mechan Eng 12:2377–2393
5. Hua Y, Nie W, Cai P, Liu YH, Peng HT, Liu Q (2018) Pattern characterization concerning spatial and temporal evolution of dust pollution associated with two typical ventilation methods at fully mechanized excavation faces in rock tunnels. Powder Technol 334:117–131. https://doi.org/10.1016/j.powtec.2018.04.059
6. Maurya T, KaremaK,Vardhan H,ArunaM, RajMG (2015) Effect of heat on underground mine workers. Procedia Earth and Planetary Science 11:491–498. https://doi.org/10.1016/j.proeps.2015.06.049
7. Ministry of Industry and Trade, 2011. National Technical Regulation on Safety in Underground Coal Mining, Hanoi Labor Publishing House.
8. Liu Shishi, Liu Shida. Nonlinear equations in physics[M]. Beijing: Peking University Press. 1994.
9. QUAN Truong Tien , Rafał ŁUCZAK1 and Piotr ŻYCZKOWSKI, 2019. Climatic hazard assessment in selected underground hard coal mines in Vietnam. Journal of the Polish Mineral Engineering Society.No2(44), p.155-163.http://doi.org/10.29227/IM-2019-02-67
10. Su HT, Zhou FB, Song XL, Qiang ZY (2017) Risk analysis of spontaneous coal combustion in steeply inclined longwall gobs using ascaled-down experimental set-up. Process Saf Environ Prot 111:1–12. doi:https://doi.org/10.1016/j.psep.2017.06.001,1
11. Su Z, Jiang Z, Sun Z (2009) Study on the heat hazard of deep exploitation in high-temperature mines and its evaluation index. Procedia Earth Planet Sci 01:414–419
12. Wu Zhongh. Mine ventilation and safety [M]. Xuzhou: China University of Mining and Technology Press, 1989, 50-245.
13. Yang X, Han Q, Pang J, Shi X, Hou D, Liu C (2011) Progress of heat-hazard treatment in deep mines. Int J Min Sci Technol 21:295–299
14. Yan Ronglin, Hou Xianwen. Mine air conditioning technology. Beijing: Coal Industry Press, 2004.
15. Zhang Y, Wan ZJ, Gu B, Zhou CB, Cheng JY (2017) Unsteady temperature field of surrounding rock mass in high geothermal roadway during mechanical ventilation. J Cent South Univ 24:374–381. https://doi.org/10.1007/s11771-017-3439-3

INŻYNIERIA MINERALNA
CZASOPISMO POLSKIEGO TOWARZYSTWA PRZERÓBKI KOPALIN

2(52)
2023